Molecular Biology of the Cell
Vol. 13, 1750–1764, May 2002

Inhibitors of COP-mediated Transport and Cholera Toxin Action Inhibit Simian Virus 40 Infection

Ayanthi A. Richards,* Espen Stang,† Rainer Pepperkok,‡ and Robert G. Parton*§

*Institute for Molecular Bioscience, Center for Microscopy and Microanalysis, and Department of Physiology and Pharmacology, School of Biomedical Sciences, University of Queensland, Queensland 4072, Australia; and ‡European Molecular Biology Laboratory, 69117 Heidelberg, Germany

Submitted December 21, 2001; Revised December 21, 2001; Accepted March 5, 2002
Monitoring Editor: Randy W. Schekman

Simian virus 40 (SV40) is a nonenveloped virus that has been shown to pass from surface caveolae to the endoplasmic reticulum in an apparently novel infectious entry pathway. We now show that the initial entry step is blocked by brefeldin A and by incubation at 20°C. Subsequent to the entry step, the virus reaches a domain of the rough endoplasmic reticulum by an unknown pathway. This intracellular trafficking pathway is also brefeldin A sensitive. Infection is strongly inhibited by expression of GTP-restricted ADP-ribosylation factor 1 (Arf1) and Sar1 mutants and by microinjection of antibodies to βCOP. In addition, we demonstrate a potent inhibition of SV40 infection by the dipeptide *N*-benzoyl-oxycarbonyl-Gly-Phe-amide, which also inhibits late events in cholera toxin action. Our results identify novel inhibitors of SV40 infection and show that SV40 requires COPI- and COPII-dependent transport steps for successful infection.

INTRODUCTION

Viruses have exploited endocytic pathways to overcome the barrier presented by the plasma membrane and enter animal cells. Although the entry of viruses via clathrin-coated pits has been extensively studied and is well understood (Marsh *et al.*, 1984), entry of viruses by alternative pathways has been less well characterized. Simian virus 40 (SV40) is a nonenveloped virus that uses an apparently unique entry route to reach the nucleus of animal cells. SV40 binds to major histocompatibility complex (MHC) class I molecules on the cell surface (Breau *et al.*, 1992) and then is observed in tight-fitting, nonclathrin-coated pits (Kartenbeck *et al.*, 1989; Anderson *et al.*, 1996; Stang *et al.*, 1997; Norkin, 1999; Parton and Lindsay, 1999). These pits are enriched in caveolin-1 but are smaller than caveolae, raising the possibility that caveolin is recruited around the virus (Stang *et al.*, 1997). Consistent with this model, the levels of caveolin-1 associated with virus-containing membranes were shown to increase with time (Stang *et al.*, 1997). Subsequently, the virus is internalized in a process that is sensitive to cholesterol-perturbing agents (Anderson *et al.*, 1996). The role of caveolin in this process is suggested by the finding that viral infection is also inhibited by dominant negative mutants of caveolin (Roy *et al.*, 1999). Viral entry apparently occurs without concomitant internalization of MHC class I (Anderson *et al.*, 1998), in a process dependent on tyrosine kinase activity (Dangoria *et al.*, 1996; Chen and Norkin, 1999; Norkin, 1999). Early electron microscopic studies suggested that the virus is then transported directly to the endoplasmic reticulum (ER) because no intermediate stations were identified (Kartenbeck *et al.*, 1989). A direct pathway between the cell surface and ER would be a novel finding, although parallels can be made to the cholesterol oxidase-induced redistribution of caveolin-1 from caveolae to the lumen of the ER (Smart *et al.*, 1994).

The virus eventually reaches the nucleus where uncoating and replication occur. At some stage in the entry pathway the SV40 virions appear to translocate across a membrane into the cytosol and then enter the nucleus via the nuclear pore complexes (Clever *et al.*, 1991; Yamada and Kasamatsu, 1993). Cytosolic microinjection of antibodies against viral proteins blocks the infection process (Nakanishi *et al.*, 1996), suggesting that the virus is actually free in the cytosol at some stage in infection but the mechanism by which trans-

Article published online ahead of print. Mol. Biol. Cell 10.1091/mbc.01–12–0592. Article and publication date are at www.molbiolcell.org/cgi/doi/10.1091/mbc.01–12–0592.

† Present address: Institute of Pathology, University of Oslo, The National Hospital, 0027 Oslo, Norway.
§ Corresponding author. E-mail address: r.parton@imb.uq.edu.au.

Abbreviations used: BFA, brefeldin A; Cbz-gly-phe-NH2, *N*-benzoyl-oxycarbonyl-Gly-Phe-amide; CT, cholera toxin; ER, endoplasmic reticulum; GFP, green fluorescent protein; GPI, glycosyl phosphatidylinositol; PDI, protein disulfide isomerase; SFV, Semliki Forest virus; SFV(cav-3), Semliki Forest virus-encoded caveolin-3; SV40, simian virus 40; T-ag, simian virus 40 T-antigen; ts-045-G, temperature-sensitive vesicular stomatitis virus glycoprotein.

location into the cytosol occurs, and the compartment involved in this process, are unknown.

Many toxins are retrogradely transported from the cell surface to the ER where translocation into the cytosol occurs. This has provided important insights into the retrograde transport process and the mechanisms involved in translocation. This process has been particularly well characterized for cholera toxin (CT). CT binds via its binding subunits to the ganglioside GM1 at the cell surface. GM1 is slightly enriched in caveolae but is present over the entire cell surface, including clathrin-coated pits (Parton, 1994). Inhibitor studies, using cholesterol-disrupting agents, have suggested that CT is internalized via caveolae (Orlandi and Fishman, 1998). However, CT is also efficiently internalized, in a cholesterol-dependent process, in cells lacking caveolae (Orlandi and Fishman, 1998). Elegant studies using chimeric toxins have shown that association with raft domains is critically important for toxic entry of CT (Wolf *et al.*, 1998). Internalization of CT and budding of caveolae have both been proposed to be dynamin dependent (Henley *et al.*, 1998; Orlandi and Fishman, 1998). After internalization CT passes to endosomes and then the *trans*-Golgi network. The toxin then arrives at the ER in a process that can be blocked experimentally by brefeldin A (BFA) and by microinjection of coatomer antibodies (Lencer *et al.*, 1993; Nambiar *et al.*, 1993; Majoul *et al.*, 1998; Girod *et al.*, 1999). This process is facilitated by a KDEL sequence in the A subunit and retrieval by the KDEL receptor (Majoul *et al.*, 1998). On reaching the ER, redox-dependent unfolding of the toxin by protein disulfide isomerase occurs (Tsai *et al.*, 2001). The A subunit is then reduced to produce the enzymatically active A^1 peptide, which is translocated to the cytosol via the Sec61 channel, identifying the rough ER as the compartment from which translocation occurs (Schmitz *et al.*, 2000).

Although recent morphological studies have suggested the involvement of a novel endosomal intermediate, termed a caveosome, in the SV40 entry pathway (Pelkmans *et al.*, 2001), the molecular mechanisms directing SV40 along this pathway and the similarities to known trafficking pathways are still unknown. Possible parallels between the SV40 pathway and that of CT are evident with both suggested to involve caveolae, the ER, and then translocation to the cytosol (Parton and Lindsay, 1999). This prompted us to examine SV40 infectious entry by using a range of manipulations previously shown to inhibit CT toxicity. We now show that SV40 infection is blocked by BFA, with inhibition at two distinct steps: the initial virus entry step and an intracellular step. Infection is also blocked by a dominant negative ADP-ribosylation factor 1 (Arf1) mutant, by a dominant negative Sar1 mutant, and by microinjection of antibodies to βCOP. These results indicate that SV40 infection either proceeds via a membrane trafficking pathway involving Golgi intermediates or requires a functional exocytic pathway. We compared the effect of these inhibitors of SV40 infection on CT entry and show that CT transport from early endosomes to the Golgi complex is inhibited by both Arf1 and Sar1 mutants. We also show that a novel inhibitor of late events in CT toxicity, the dipeptide *N*-benzoyl-oxycarbonyl-Gly-Phe-amide (Cbz-gly-phe-NH2), blocks late intracellular steps in SV40 infection, providing new insights into this novel virus entry pathway.

MATERIALS AND METHODS

Antibodies and Reagents

The expression plasmids encoding Arf1(Q71L) (Pepperkok *et al.*, 1998; Girod *et al.*, 1999), Sar1(H79G) (Aridor *et al.*, 1995; Pepperkok *et al.*, 1998), and green fluorescent protein (GFP)-tagged temperature-sensitive vesicular stomatitis virus glycoprotein (ts-045-G) (Scales *et al.*, 1997), and affinity-purified anti-βCOP (EAGE) (Pepperkok *et al.*, 1993) have been described previously. Anti-βCOP (EAGE) antiserum (used for immunofluorescence labeling) and mouse monoclonal antibodies to protein disulfide isomerase (PDI) (Pizarro-Cerda *et al.*, 1998) were kind gifts of Drs. Rohan Teasdale and Jenny Stow, respectively (Institute for Molecular Bioscience, Queensland, Australia). Rabbit neutralizing antiserum to SV40 (Butel *et al.*, 1984) from Dr. Janet Butel (Department of Molecular Virology and Microbiology, Baylor College of Medicine, Houston, TX), affinity-purified anti-p23 (Rojo *et al.*, 1997) from Dr. Manuel Rojo (Department of Biochemistry, University of Geneva, Switzerland), human antiserum to EEA1 from Dr. Ban-Hock Toh (Melbourne, Australia), and murine antigiantin (Linstedt and Hauri, 1993) from Dr. Hans-Dieter Soeling (Gottingen, Germany) were also generous gifts. Murine monoclonals against caveolin-3 (Transduction Laboratories, Lexington, KY), GM130 (Transduction Laboratories), and SV40 T-antigen (PharMingen, San Diego, CA) were commercially obtained. Brefeldin A, Cbz-gly-phe-NH2, Cbz-gly-gly-NH2, fluorescein isothiocyanate (FITC)-conjugated CT-B subunit, unlabeled holotoxin, and antiserum to CT were obtained from Sigma-Aldrich (St. Louis, MO). 4,6-Diamidino-2-phenylindole (DAPI) and Texas Red-conjugated transferrin were from Molecular Probes (Eugene, OR). Media and cell culture reagents were purchased from Invitrogen (Carlsbad, CA) or BioWhittaker (Walkersville, MD).

Cell Culture and Viral Infections

Vero cells (African green monkey kidney cells, ATCC CCL 81) and CV1 cells (African green monkey kidney cells, ATCC CCL 70) were maintained in DMEM supplemented with 10% (vol/vol) serum supreme (BioWhittaker) and 2 mM L-glutamine plus or minus penicillin (100 U/ml) and streptomycin (100 μg/ml). Stocks of recombinant Semliki Forest virus (SFV) encoding caveolin-3 (from Dr. Elina Ikonen, National Public Health Institute, Helsinki, Finland) were diluted into serum-free medium containing 2 mM L-glutamine and 0.2% bovine serum albumin before addition to cells. After 1 h of infection at 37°C, cells were washed and infection allowed to proceed for 5 h or more before fixation and immunolabeling for caveolin-3 to detect successfully infected cells. Preparation of SV40-containing supernatant from infected CV1 and Vero cultures and subsequent use of these viral stocks in infection experiments was as described previously (Stang *et al.*, 1997). Stocks used to generate SV40 supernatants were a generous gift from Dr. Jurgen Kartenbeck (Division of Cell Biology, German Cancer Research Center, Heidelberg, Germany).

Microinjection

Antibody samples for microinjection were each prepared as previously described in the cited references. Purified rabbit IgG (Sigma-Aldrich) solubilized in 10 mM KH_2PO_4, pH 7.2, and 75 mM KCl microinjection buffer (Henley *et al.*, 1998) was injected at 10 mg/ml as a control. Plasmid DNA for microinjection was purified on a cesium chloride gradient and injected into the nucleus of cells at 50–100 μg/ml. Capillary microinjection of antibodies and DNA into cells was performed using a computer-assisted, automated microinjection system (CompiC INJECT, AIS2; Cellbiology Trading, Hamburg, Germany) by using microcapillaries pulled from thin-wall borosilicate glass capillaries (1.2-mm outer diameter; 0.94-mm inner diameter) (Clark Electromedical Instruments, Pangbourne Reading, England) by a Flaming/Brown P-97 micropipette puller (Sutter, Novato, CA). Cells to be injected were plated onto small glass

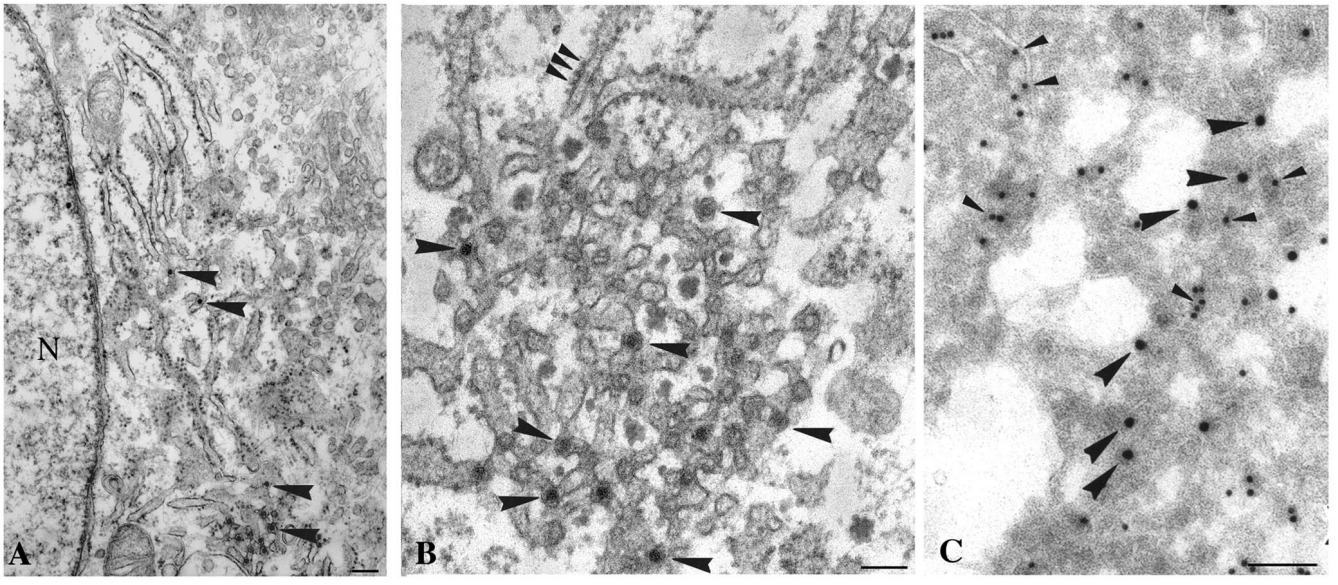

Figure 1. Electron microscopic localization of SV40 in PDI-positive subdomain of ER. Vero cells were incubated with SV40 for 18 to 21 h at 37°C before fixation and processing for either epon embedding (A and B) or frozen sectioning (C). (A and B) SV40 accumulates in a domain of the rough ER. Virus particles (large arrowheads) are in smooth-membraned areas of the rough ER; ribosomes (small arrowheads in B) are evident on cisternae connected to the SV40-containing structures. (C) Frozen section labeled for SV40 (large gold, large arrowheads) and for PDI (small gold, small arrowheads) showing colocalization of the virus with the ER marker. N, nucleus. Bars, 200 nm.

coverslips and injected at room temperature (RT) in Hanks' medium containing 0.75 mg/ml bicarbonate and 10 mM HEPES, pH 7.4. Cells were allowed to recover for 0.5–4 h postinjection (or 5 h for expression of injected cDNA) in penicillin-streptomycin–containing medium at 37°C before subsequent manipulations.

Immunofluorescence and Electron Microscopy

Experiments requiring immunolabeling with the monoclonal antibody to SV40 T-antigen were fixed in 100% methanol for 5 min at −20°C. Microinjection experiments requiring this fixation were often first fixed with 4% paraformaldehyde (PFA) in phosphate-buffered saline (PBS) at RT for 20 min and subsequently fixed with 100% methanol as described above. This reduced the washing out of the injected antibody by methanol fixation. All other experiments were fixed only with 4% PFA in PBS at RT for 20 min. Processing of cells for immunofluorescence analysis was as follows. PFA-fixed cells were permeabilized in 0.1% saponin in PBS for 10 min before subsequent incubation in 50 mM NH_4Cl in PBS for 10 min (to quench aldehyde groups) and in blocking solution (composed of 0.2% bovine serum albumin and 0.2% fish skin gelatin in PBS) for 20 min at RT. A 30-min incubation in blocking solution containing primary antibodies was followed by 4 × 5-min PBS washes before incubation in blocking solution containing fluorescently tagged secondary antibodies for 20 min. After further 4 × 5-min PBS washes, the cells were rinsed in water and mounted in Mowiol mounting medium. In experiments requiring nuclear staining, the cells were incubated in 1 μg/ml DAPI in PBS for 2 min just before rinsing and mounting. Cells fixed with methanol did not require saponin permeabilization. Experiments were viewed and photographed with an Olympus BX60 microscope connected to a Daige charge-couple device camera image capture system. Immunofluorescence images were prepared using Adobe Photoshop 5.0 (Adobe Systems, Mountain View, CA). Cells were processed for electron microscopy according to Stang *et al.* (1997).

Quantitation of Viral Infection

Infection efficiencies of 20 or more antibody-injected cells and 40 or more transfected cells per experiment were quantified. For drug treatment and temperature-sensitivity experiments, efficiency of infection was quantified from 100 or more cells from each treatment.

RESULTS

Surface-to-ER Traffic of SV40

SV40 has been shown to be internalized by caveolae and then to reach a subdomain of the ER. The molecular machinery and sorting mechanisms by which the virus reaches the compartment are presently unknown.

We first examined the nature of the SV40-containing compartment by using both plastic sections and immunolabeling. Epon sections of cells incubated with SV40 for 21 h revealed the virus in reticular, smooth-membraned areas of the ER connected to ribosome-studded rough ER membranes (Figure 1, A and B). The membrane is closely apposed to the surface of the viral particles, suggesting that the virus remains bound to the lumenal surface of the membrane. Ultrathin frozen sections of these cells were labeled with antibodies to the virus together with antibodies to a *cis*-Golgi marker, p23, or to a marker of the ER, PDI. The virus-containing membranes were negative for the *cis*-Golgi/intermediate compartment labeled by antibodies to p23 (our unpublished data) but were labeled by antibodies to PDI (Figure 1C). Although the majority of the virus particles was observed in these very prominent enlarged ER domains, virus particles were occasionally observed in proximity to the Golgi complex, and possibly in Golgi-associated membranes (our unpublished data), raising the possibility

that virus may transiently associate with these compartments during infection.

Brefeldin A Inhibits Entry and Postentry Trafficking of SV40

The above-described observations prompted us to further examine the possibility that SV40 passes transiently through the Golgi compartment in a similar manner to many bacterial toxins, which also follow an endocytic route to the ER. Because transient intermediates in infection may be difficult to identify morphologically and the viral infection process is relatively unsynchronized, we chose to use defined membrane trafficking inhibitors together with assays of infection to further delineate the trafficking pathway.

We first examined the possible involvement of the Golgi complex in the SV40 trafficking pathway by using the fungal metabolite BFA. This drug inhibits guanine nucleotide exchange on the small GTPase Arf1 (Jackson and Casanova, 2000), an adapter protein responsible for recruitment of COPI coats onto endosomal and biosynthetic membranes. The result is an inhibition of anterograde transport from ER to Golgi complex (Misumi *et al.*, 1986) and a concomitant tubulation and fusion of the Golgi with the ER (Lippincott-Schwartz *et al.*, 1989; Scheel *et al.*, 1997). Consequently, BFA has been widely used to inhibit both anterograde and retrograde transport between the Golgi complex and ER. Vero cells were pretreated for 3 h with BFA and then incubated with SV40 plus BFA for 21 h before fixation and immunolabeling for the virus-encoded T-antigen (T-ag). As shown in Figure 2, BFA is a potent inhibitor of SV40 infection. With concentrations as low as 0.1 μg/ml we observed 99% inhibition of infection (Figure 2E). These relatively low doses of 0.1 and 0.5 μg/ml BFA were found to be effective in disrupting Golgi morphology within 1 and 3 h of treatment, respectively (Figure 2, A and B).

To determine the stage of the infectious entry pathway that was affected by BFA, Vero cells were exposed to a 3-h pulse treatment of 0.1 μg/ml BFA at various time points into SV40 infection at 37°C. Fixation and immunolabeling for T-ag after the 21-h infection period revealed a clear inhibition of SV40 infection when BFA was applied at early stages of viral infection (Figure 2E). To examine the possibility that BFA blocks viral entry, we made use of a neutralizing anti-SV40 antibody, which inactivates surface virus. Addition of the neutralizing antibody to cells incubated with the virus at 4°C with no warming step to allow internalization caused a complete block of infection (our unpublished data). Vero cells cultured in the presence or absence of 0.5 μg/ml BFA for 1 h at 37°C were incubated with SV40 plus or minus BFA on ice for 1 h and then at 37°C for 2 h to allow infection to occur. The cells were then incubated in SV40 neutralizing antibody for 30 min and washed to remove BFA. A further 46 h of infection at 37°C was followed by fixation and immunofluorescence labeling for T-ag. Quantitation of SV40 infection efficiency revealed a substantially greater sensitivity of SV40 infection to the neutralizing antibody in BFA-treated cells compared with untreated cells, indicating a trapping of the virus at the cell surface by BFA (Figure 2F). Thus, it was apparent that the first effect of BFA on SV40 infection was the inhibition of initial viral entry. Consistent with this, treatment with 0.3 μg/ml BFA and incubation with the virus for 21 h showed SV40 immunolabeling only at the periphery of cells, unlike the pattern observed in untreated controls (Figure 2, C and D). Dual immunolabeling for caveolin-1 and SV40 revealed no significant colocalization (our unpublished data). Similar results were obtained in cells transiently transfected with caveolin-1-YFP with no colocalization of peripheral SV40 labeling with caveolin-1-YFP (our unpublished data). Epon sections of these cells revealed virus particles in tight-fitting, surface-connected invaginations indistinguishable from those seen in untreated cells at early time points. In accordance with the immunofluorescence data, few virus particles were observed intracellularly (Figure 2G).

To investigate whether BFA also inhibits postsurface trafficking steps, Vero cells were incubated with SV40 for 2 h at 37°C in the absence of BFA to allow viral infection to proceed past the initial internalization step. Any virus remaining at the cell surface was then inactivated with neutralizing antibody and the cells incubated in either the presence or absence of 0.5 μg/ml BFA for the remaining 20 h of infection. Quantitation revealed a strong inhibition of infection in BFA-treated cells compared with untreated controls, showing inhibition of an internal step in SV40 infection (Figure 2H).

We conclude that the initial entry step of SV40 entry is BFA sensitive. In addition, SV40 infection involves a second postentry BFA-sensitive step, possibly involving endosomes and/or the Golgi complex.

SV40 Entry Is Inhibited at 20°C

Although BFA is best known for its inhibitory effect on transport between ER and Golgi complex, it has also been shown to inhibit early endosome-to-Golgi complex traffic (e.g., of endocytosed Shiga toxin; Mallard *et al.*, 1998). To determine whether SV40 is internalized to early endosomes, we made use of the observation that exit from the early endosome is blocked at 20°C (Griffiths *et al.*, 1988). Vero cells were infected with SV40 at 20°C for 4 h. Fixation and immunolabeling for the virus revealed a striking loss of staining for the virus (our unpublished data). To confirm this apparent failure of the virus to be internalized at 20°C, we again used the SV40 neutralizing antibody assay. Vero cells were infected with the virus either at 20 or at 37°C for 4 h. Subsequent exposure of the cells to the neutralizing antibody for 30 min was followed by incubation at 37°C for a further 24 h before fixation and immunolabeling for T-ag. Quantitation of infection efficiency revealed a much greater sensitivity of the virus to the neutralizing antibody after a 4-h infection at 20°C than after infection at 37°C (Figure 3). We conclude that initial entry of SV40 is sensitive to both BFA and incubation at 20°C.

CT Exit from Early Endosomes Is Inhibited by BFA and by Incubation at 20°C

We next examined the effects of these treatments on a well-characterized retrograde transport pathway. CT is efficiently transported to the ER via the Golgi complex (see INTRODUCTION). We have used either FITC-labeled CT-B (CT-B-FITC), which is transported to the Golgi, or immunolabeling for the holotoxin, which is transported to the ER (Lencer, 2001). Vero cells allowed to bind and internalize the FITC-

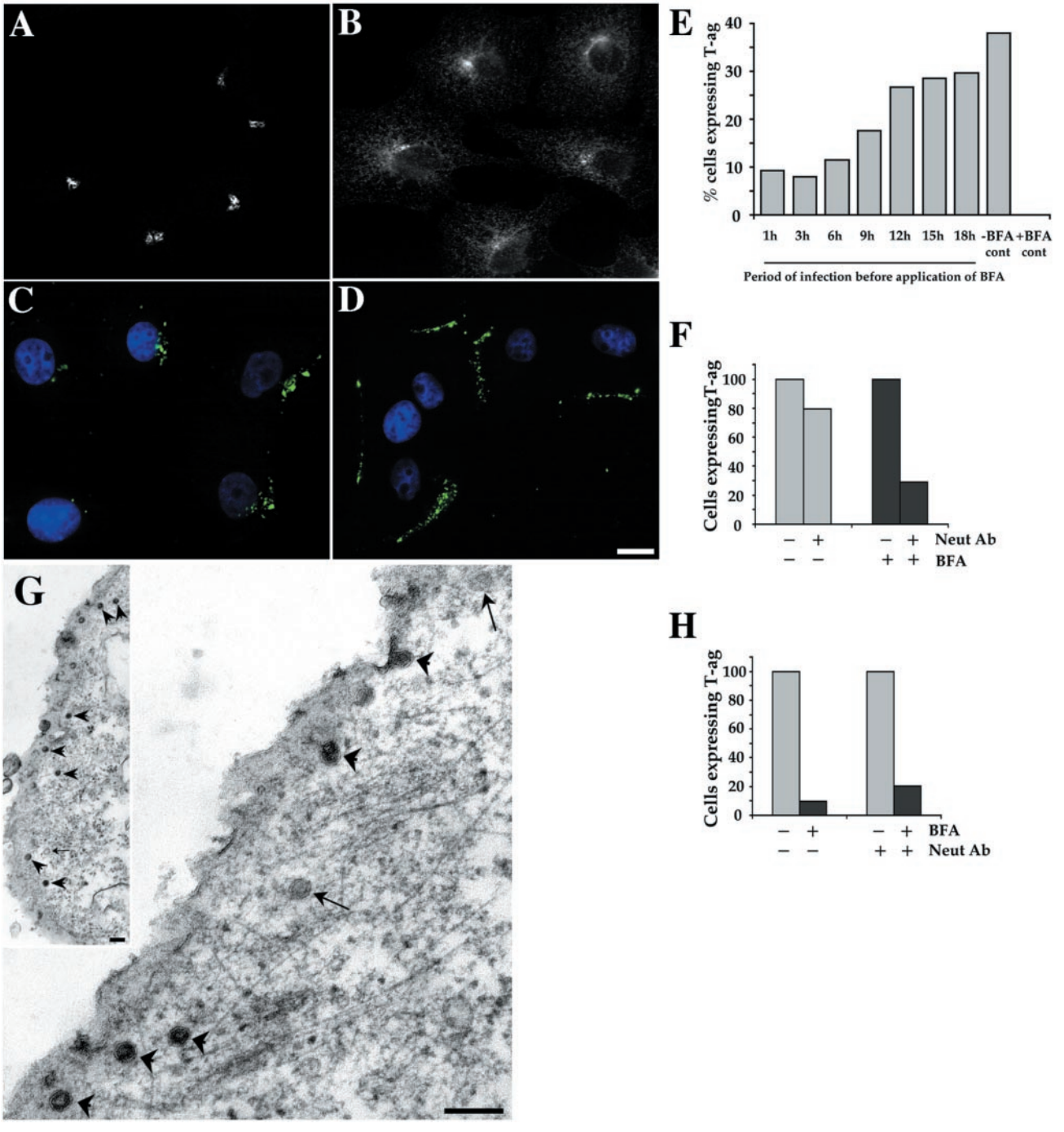

Figure 2. BFA sensitivity of early events in SV40 infection. Treatments of 0.1 μg/ml BFA for 3 h (B) were found to disrupt the Golgi complex of Vero cells (cf. untreated cells in A) as revealed by immunolabeling for the Golgi marker giantin. In Vero cells treated with 0.1 μg/ml BFA for 3 h and subsequently infected with SV40 for 21 h in the continued presence of the drug, a potent inhibition of viral infection was observed (E; +BFA control). Immunolabeling for SV40 (green) and nuclear staining with DAPI (blue) revealed an accumulation of the virus at the periphery of cells treated with BFA (D), a pattern clearly different from that observed in untreated cells (C). (E) When the 3-h BFA treatment was applied at various time points after the commencement of infection, a sensitivity to the drug of early but not later events in SV40 infection was evident. A representative experiment is shown. (F) BFA inhibits SV40 internalization. Vero cells cultured in 0.5 μg/ml BFA for 1 h were allowed to internalize SV40 for 2 h at 37°C in the presence or absence of the drug. Subsequent exposure of the cells to an SV40 neutralizing antiserum allowed inactivation of all surface-exposed virus before a further 46 h of infection in the absence of the drug. Fixation and immunolabeling for T-ag revealed a substantially greater sensitivity of virus infection to the neutralizing antiserum in BFA-treated cells compared with untreated controls. A representative experiment is shown. Infection efficiencies are shown normalized to those of controls not

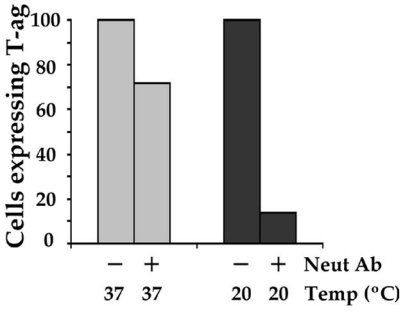

Figure 3. SV40 internalization is inhibited at 20°C. Vero cells were infected with SV40 for 4 h at either 20 or 37°C before neutralizing surface-exposed virus with SV40 neutralizing antiserum. After subsequent incubation at 37°C for a remaining 24 h, the cells were fixed and immunolabeled for T-ag. Quantitation of infection efficiency revealed a much greater sensitivity of the virus to the neutralizing antibody after infection at 20°C than after infection at 37°C. Infection efficiencies are shown normalized to controls not exposed to the neutralizing antiserum. A representative experiment is shown.

labeled B subunit of the toxin at 20°C showed no inhibition of toxin accumulation in early endosomes (Figure 4, A–C). Similarly, Vero cells pretreated for 1 h with 0.5 μg/ml BFA also internalized the toxin to early endosomes (Figure 4, D–F). In cells exposed to BFA for a 21-h period comparable with that used in SV40 infection experiments, internalization of CT was still observed, although a greater intensity of plasma membrane fluorescence, possibly indicating a decrease in uptake, was detected (our unpublished data).

Although BFA and a 20°C incubation had little effect on internalization of CT-B, subsequent transport to the Golgi was completely inhibited by both treatments. Even after a 1-h incubation at 20 or 37°C in the presence of BFA, the toxin failed to reach the Golgi (Figure 4, A–F). In cells exposed to BFA (Figure 4, D–I) the toxin accumulated in sorting endosomes and tubulated recycling endosomes identified by colocalization of cointernalized Texas Red-labeled transferrin with CT-B-FITC (Figure 4, G–I). We conclude that the sensitivity of SV40 entry to both BFA and incubation at 20°C is in contrast to other known endocytic pathways, including that of the putative caveolae marker CT (Lencer *et al.*, 1993; Nambiar *et al.*, 1993) and suggests that SV40 uses a novel entry pathway.

Figure 2 (cont). exposed to the neutralizing antiserum. (G) Epon sections of Vero cells cultured in 0.3 μg/ml BFA for 3 h and then infected with SV40 for 21 h in the presence of the drug. Thin sections revealed an accumulation of virus particles at the cell surface as shown at low magnification in the inset. The virus accumulates in apparently normal caveolae-like invaginations (arrowheads). Empty caveolae are also apparent (arrows). (H) BFA inhibits intracellular trafficking of SV40. Vero cells were infected with SV40 for 2 h at 37°C before exposure to the neutralizing antiserum. Subsequent culture with or without 0.5 μg/ml BFA for the remaining 20 h of infection was followed by fixation and immunolabeling for T-ag. Cell counts revealed a strong inhibition of infection in BFA-treated cells compared with untreated controls. Infection efficiencies are shown normalized to those of untreated controls. A representative experiment is shown. Bars, 20 μm (A–D) and 100 nm (G).

Inhibition of SV40 Infection by Microinjected Antibodies to βCOP and by Expression of Arf1 and Sar1 Mutants

The sensitivity of a postsurface SV40 trafficking step to BFA treatment raised the possibility of Golgi complex involvement in the viral entry pathway. Inhibition of retrograde traffic between the Golgi complex and ER has been convincingly demonstrated by microinjection of an antibody to βCOP, a component of the coatomer complex of COPI-coated vesicles. Microinjection of anti-βCOP (EAGE) (Pepperkok *et al.*, 1993) was found to inhibit COPI-mediated retrograde transport of the KDEL receptor and of ERGIC-53, both molecules that constitutively cycle between the ER and Golgi complex (Girod *et al.*, 1999). Retrograde traffic of endocytosed CT-A subunit has also been found to be inhibited by anti-βCOP injection (Majoul *et al.*, 1998; Girod *et al.*, 1999). Vero cells were microinjected with anti-βCOP antibodies. Three to four hours later the cells were infected with SV40 for 21 h before fixation and immunolabeling for the microinjected antibody and T-ag. The microinjected antibodies showed cytosolic labeling and strong Golgi staining (Figure 5A). Quantitation of infection efficiency revealed a strong inhibition of viral infection in microinjected cells, compared with surrounding uninjected cells (Figure 5B), showing that the anti-βCOP antibody is a potent inhibitor of SV40 infection.

As a second independent method to inhibit COPI-mediated transport we used overexpression of a GTPase-deficient Arf1 mutant (Q71L). This mutant has previously been shown to inhibit COPI-dependent transport in the early secretory pathway (Dascher and Balch, 1994) and also to inhibit sorting and concentration of cargo molecules into COPI-coated vesicles in vitro (Lanoix *et al.*, 1999). Vero cells were microinjected with either a mixture of Arf1(Q71L) and GFP expression plasmids or the GFP plasmid alone (as a control). After 5 h to allow expression of proteins the cells were incubated with SV40. Expression of Arf1(Q71L) in GFP-expressing cells injected with both plasmids was verified by immunolabeling the cells for βCOP. A clear disruption or complete disappearance of the Golgi βCOP labeling pattern in cells showing high levels of GFP expression was observed in cells injected with both plasmids but not in cells injected only with the GFP construct (Figure 6, A–D). Quantitation of infection efficiency revealed a potent inhibition of SV40 infection in Arf1(Q71L)-expressing cells compared with neighboring nonexpressing cells. No such inhibition was observed in cells expressing GFP alone (Figure 6E).

In addition to their effects on COPI-mediated retrograde transport between the Golgi and ER, the dominant negative Arf1 mutant and microinjected βCOP antibody could also be affecting events early in endocytosis because Arf1 and COP proteins have been implicated in endosomal trafficking (Aniento *et al.*, 1996; Daro *et al.*, 1997; Gu *et al.*, 1997; Gu and Gruenberg, 2000; Jackson and Casanova, 2000). To determine whether disruption of ER/Golgi transport could be responsible for inhibiting viral infection, we examined the effect of a selective inhibitor of ER/Golgi transport on SV40 infection by expression of the

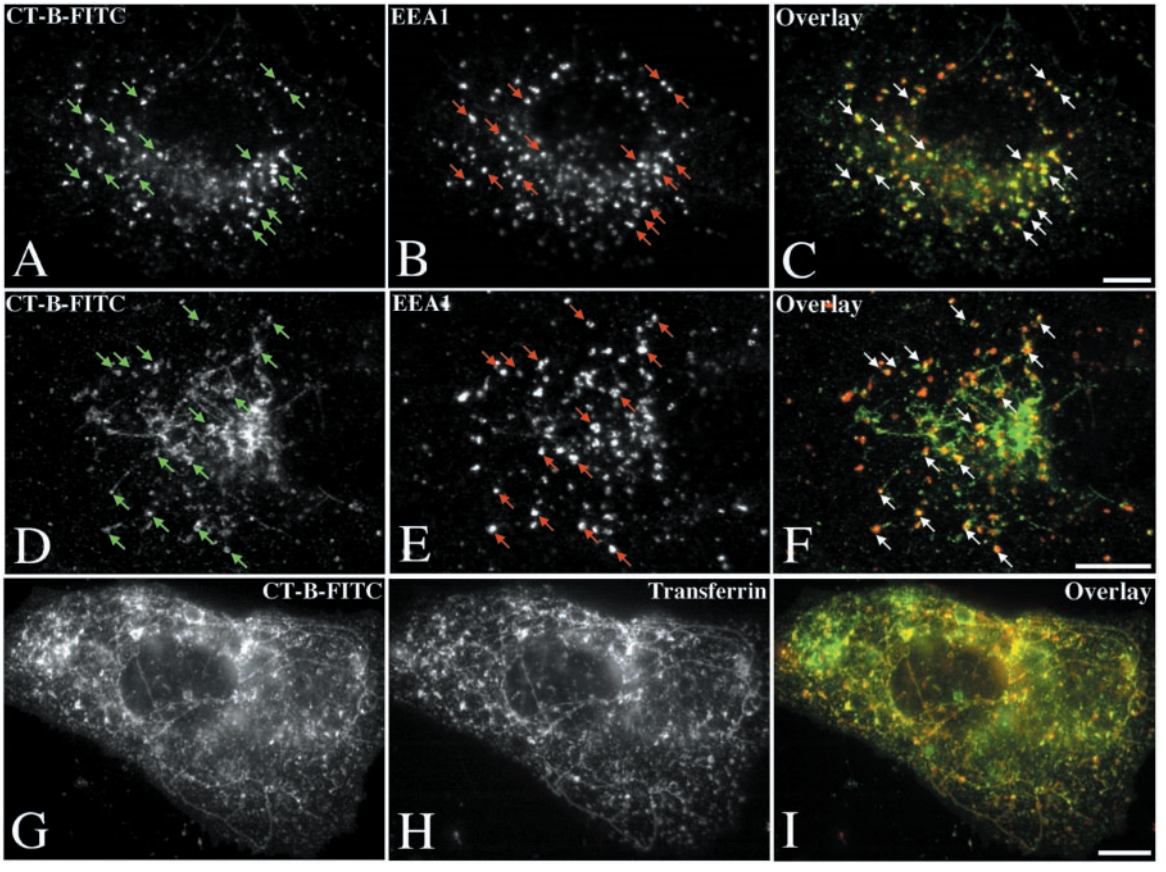

Figure 4. Early endosome-to-Golgi transport of CT-B is inhibited at 20°C and by BFA. Incubation of Vero cells in 0.5 μg/ml CT-B-FITC for 1 h at 20°C resulted in accumulation of the toxin in EEA1-positive early endosomes (arrows) and a failure of the toxin to reach the Golgi complex (A–C). Similarly, pretreatment with 0.5 μg/ml BFA for 2 h before subsequent internalization of CT-B-FITC in the continued presence of BFA resulted in toxin delivery to EEA1-positive early endosomes (arrows) without subsequent arrival at the Golgi complex even after 1 h at 37°C (D–F). In BFA-treated cells, CT-B-FITC was also observed in a tubulated compartment identified as the recycling endosome by colocalization with cointernalized transferrin-Texas Red (G and I). Bars, 10 μm.

GTP-restricted mutant of Sar1, Sar1(H79G) (Aridor *et al.*, 1995). We observed that cells coinjected with expression plasmids for GFP and Sar1(H79G) showed significant inhibition of SV40 infection (Figure 6F). Use of a temperature sensitive form of vesicular stomatitis virus glycoprotein (ts-045-G) confirmed that Sar1(H79G) and also Arf1(Q71L) were potently inhibiting anterograde transport in this system (Figure 7). These results show a direct

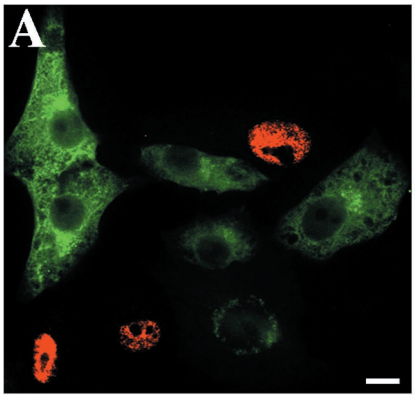

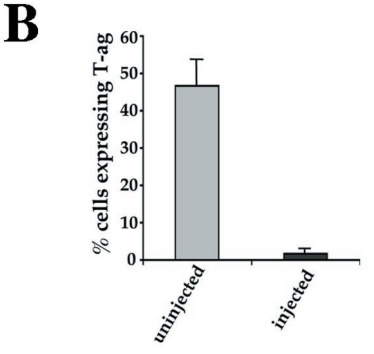

Figure 5. Inhibition of SV40 infection by microinjection of a βCOP antibody. Vero cells were microinjected with the βCOP antibody, anti-EAGE, and subjected to SV40 infection. Fixation and dual immunolabeling for the viral nuclear antigen T-ag (red) and the microinjected antibody (green) allowed detection of infected and injected cells, respectively (A). Cell counts revealed a dramatic inhibition of SV40 infection by the βCOP antibody (B). The mean and SEM of three independent experiments are shown. Bar, 20 μm.

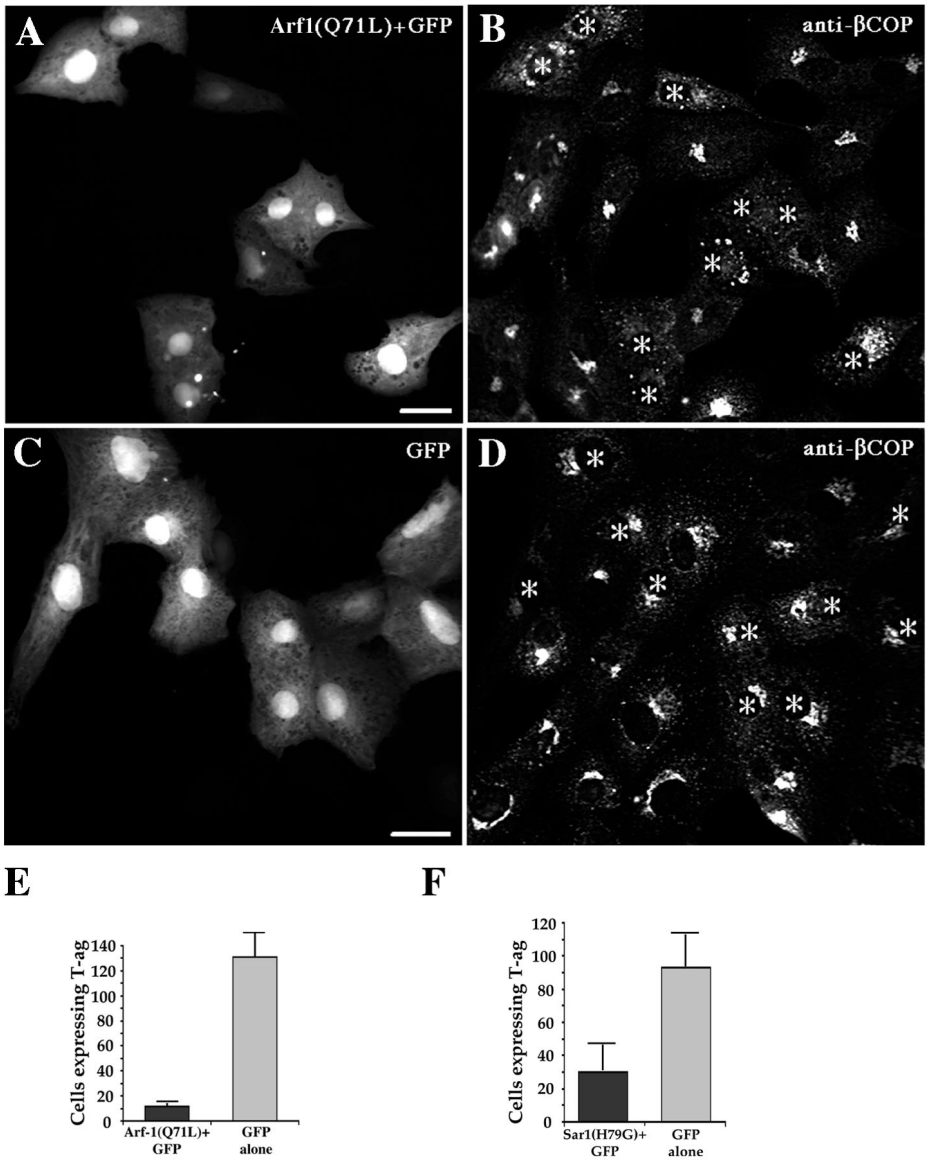

Figure 6. Inhibition of SV40 infection by Arf1(Q71L) and Sar1(H79G). Vero cells were injected with either a mixture of Arf1(Q71L) and GFP expression plasmids (A) or the GFP plasmid alone (C) and incubated for 5 h to allow protein expression to occur. Immunolabeling for βCOP (B and D) revealed an obvious disruption or complete absence of the Golgi βCOP labeling pattern in cells expressing GFP and Arf1(Q71L) (A and B) but not in cells expressing only GFP (C and D). Subjection of these cells to SV40 infection and quantitation of infection efficiency revealed a potent inhibition in Arf1(Q71L)-transfected cells compared with cells expressing GFP alone (E). A significant inhibition of SV40 infection was also elicited by a GTPase-deficient Sar1 mutant in a similar experiment (F). The graphs show the mean and SEM of three independent experiments. Infection efficiencies of transfected cells have been normalized to those of surrounding untransfected cells. Bars, 40 μm.

or indirect role for Arf1, Sar1, and COP-dependent trafficking steps in SV40 infection.

Inhibition of CT Transport to Golgi by Arf1(Q71L) and Sar1(H79G)

To further compare the CT and SV40 trafficking pathways, we examined the effect of the above-mentioned inhibitors on trafficking of CT-B to the Golgi complex or of CT holotoxin to the ER. Cells microinjected with plasmids encoding Arf1(Q71L) and Sar1(H79G) were incubated for 5 h and then allowed to bind and internalize CT-B-FITC for 40 min. A clear inhibition of toxin arrival at the Golgi was observed. The toxin was, however, internalized to early endosomes, although an obvious increase in intensity of cell-surface signal indicated a slight inhibition of entry (Figure 8). A similar inhibition of CT internalization was elicited by microinjection of the anti-βCOP antibody (EAGE) (our unpublished data).

We then examined trafficking of CT holotoxin to the ER. Untreated cells showed that CT reached the ER in 2 h as judged by immunofluorescence (Figure 9). Vero cells were injected with the above-mentioned constructs and protein expression was prevented by incubation with cycloheximide for 4 h. The cells were then allowed to bind and internalize CT holotoxin at 20°C for 1 h in the absence of cycloheximide. After subsequent incubation at 37°C for a further 2 h, the cells were fixed and immunolabeled for CT. This protocol allowed initial internalization of CT to endosomes at 20°C in the absence of mutant protein, but subsequent transport to the Golgi and ER at 37°C occurred in the presence of newly synthesized mutant pro-

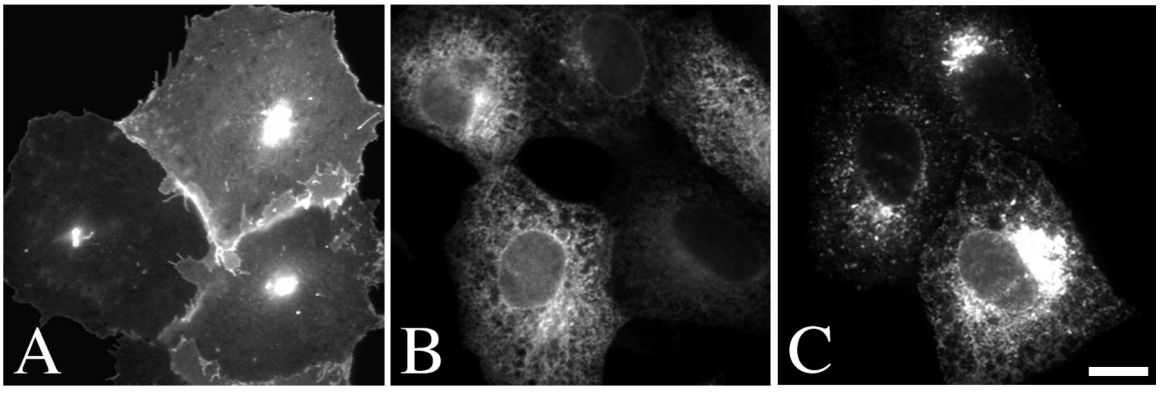

Figure 7. Exocytic transport of ts-045-G is inhibited by Sar1(H79G) and Arf1(Q71L). Vero cells were injected with GFP-tagged ts-045-G expression plasmid alone (A), or with a mixture of ts-045-G and either Sar1(H79G) (B) or Arf1(Q71L) (C) expression plasmids. Subsequent incubation at the restrictive temperature (39.5°C) for 3 h allowed expression of the mutant proteins and accumulation of ts-045-G in the ER (our unpublished data). A further 3-h incubation at the permissive temperature (31°C) resulted in delivery of ts-045-G to the plasma membrane in cells expressing this mutant alone (A). However, in cells expressing either Sar1(H79G) (B) or Arf1(Q71L) (C), ts-045-G remained trapped in the ER and in perinuclear aggregates and was never seen to reach the plasma membrane. Bar, 20 μm.

teins. As shown in Figure 9, the mutant proteins caused inhibition of transport to the ER with toxin accumulating in early endosomes (identified by colocalization with EEA1; our unpublished data) or perinuclear putative Golgi elements.

The inhibition of CT transport out of endosomes and to the Golgi by Arf1(Q71L) is in full accord with the previously described effect of BFA and could be explained by an Arf1/COPI-mediated transport step between endosomes and the Golgi complex. However, the similar inhibition by Sar1(H79G) can only be due to either disruption of the Golgi or a reliance of this endocytic pathway on a functional exocytic pathway.

Inhibition of SV40 Infection by Cbz-gly-phe-NH2

To further compare SV40 infectious trafficking with the trafficking of CT to the ER and then cytosol, we investigated the effect of a recently described inhibitor of CT toxicity. The dipeptide benzyloxycarbonyl Cbz-gly-phe-NH2 causes a potent block in the late stages of toxin action and has no effect on the initial toxin entry step (De Wolf, 2000). This agent thus provides an important tool for comparing late stages in SV40 trafficking with those of CT.

Vero cells were preincubated for 1 h with 2 mM Cbz-gly-phe-NH2 or an inactive anolog, Cbz-gly-gly-NH2. The cells were then incubated for 21 h with SV40 in the continued presence of the same drug. Quantitation of T-ag expression efficiency revealed a potent inhibition of infection by Cbz-gly-phe-NH2 (Figure 10A). In contrast, the inactive analog Cbz-gly-gly-NH2 had no effect at the same concentration (Figure 10A). Infection was similarly inhibited in cells allowed to internalize the virus for 4 h before inactivation of surface-exposed SV40 (using the neutralizing antibody) and simultaneous exposure to the inhibitory dipeptide. This confirms an inhibition of the virus postentry (Figure 10D).

To assess whether the drug is specific for a retrograde trafficking pathway such as that followed by SV40 or CT, we examined its effects on infection by an enveloped virus, SFV. This virus enters cells by clathrin-mediated endocytosis and requires delivery to acidic endosomes for translocation to the cytosol and productive infection (Marsh *et al.*, 1984). When Vero cells were exposed to recombinant SFV in the presence of the drug, no inhibitory effects on infection and expression of the SFV-encoded protein, caveolin-3 [SFV(cav-3)], were observed (Figure 10B).

As shown for the inhibition of CT toxicity, the effect of Cbz-gly-phe-NH2 on SV40 infection was found to be quickly reversible. Cells pretreated for 1 h before washing out the drug and infection with SV40 showed no inhibition of infection compared with untreated controls (our unpublished data). This suggests no lasting effects of the 1-h pretreatment. Furthermore, as observed for CT internalization, the block in SV40 infection appeared to be in late steps of the infectious pathway. A 21-h SV40 infection in the presence of the drug was followed by various periods of incubation in the absence of the drug before fixation and immunolabeling for T-ag. The percentage infection of treated cells stayed very low for the first 3 h after washing out the drug but began to recover after 6 h and reached control levels after 9 h (Figure 10C). This time period is shorter than that required for infection if virus is added to the outside of the cells and shows that the virus accumulates at a late stage in the infectious entry pathway. In keeping with this, electron microscopy of plastic sections revealed no detectable difference in the number of viral particles reaching ER cisternae in inhibitor- and control-treated cells (our unpublished data).

Finally, we examined CT trafficking in Cbz-gly-phe-NH2–treated cells. No inhibition of CT-B-FITC arrival to the Golgi was detected in inhibitor-treated cells, suggesting that only late events in the toxic entry pathway are affected (Figure 11).

In conclusion, we have identified a potent new reversible inhibitor of SV40 infection that acts at a late stage in the infectious entry process. This makes Cbz-gly-phe-NH2 an invaluable tool for detailed characterization of these trafficking pathways.

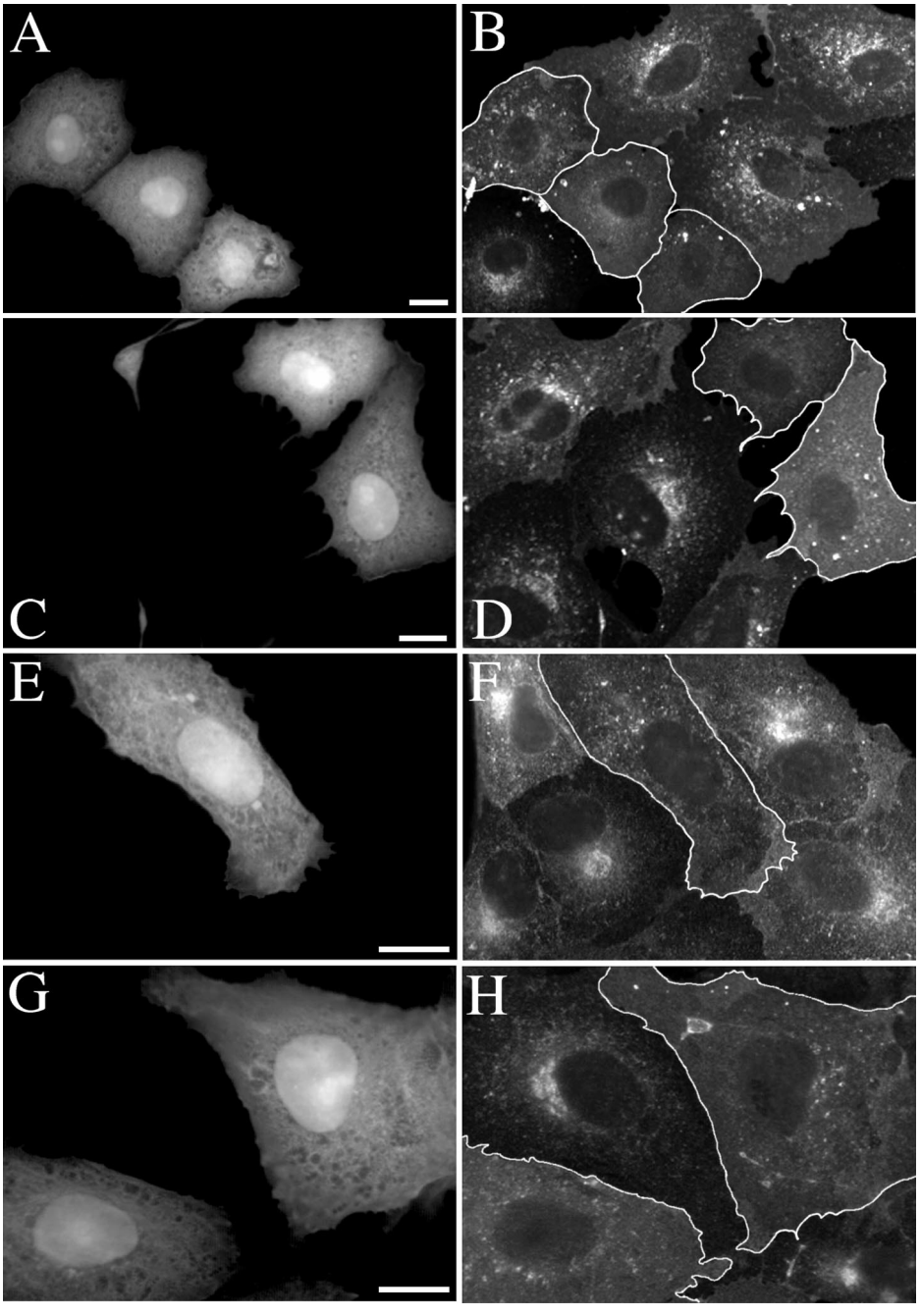

Figure 8. CT transport to the Golgi complex is inhibited by Arf1(Q71L) and Sar1(H79G). Vero cells were injected with a mixture of GFP and either Arf1(Q71L) (A–D) or Sar1(H79G) (E–H) expression plasmids. After a 5-h period of protein expression, the cells were allowed to bind either CT-B-FITC or unlabeled holotoxin and internalize for 40 min at 37°C. Injected cells (identified by GFP expression shown in A, C, E, and G) displayed internalization of the toxin to early endosomes but not to the Golgi (outlined cells in B, D, F, and H). An apparent accumulation of toxin at the cell surface of injected cells was also often noted and may reflect a slight reduction in initial internalization. Bars, 20 μm.

DISCUSSION

The present study provides new insights into the pathway by which a simple nonenveloped virus, SV40, passes from the cell surface to its site of replication, the nucleus. This pathway involves transport from cell surface caveolae to a subdomain of the rough ER. We have examined this pathway morphologically and then proceeded to use specific inhibitors to disrupt the infectious entry pathway. We now show that the initial step in virus entry displays unique characteristics, being blocked by BFA and by incubation of cells at 20°C. We have also shown that the virus uses a pathway reliant on Arf1/COPI and Sar1 function to reach the ER. Finally, we have identified a novel inhibitor of viral infection, the dipeptide Cbz-gly-phe-NH2, known to block CT toxicity. These studies give fundamental new insights into the molecular mechanisms involved in this novel virus entry pathway.

Molecular Characterization of SV40 Entry

SV40 infection proceeds via binding of the virus to MHC class I molecules on the cell surface (Breau *et al.*, 1992) and

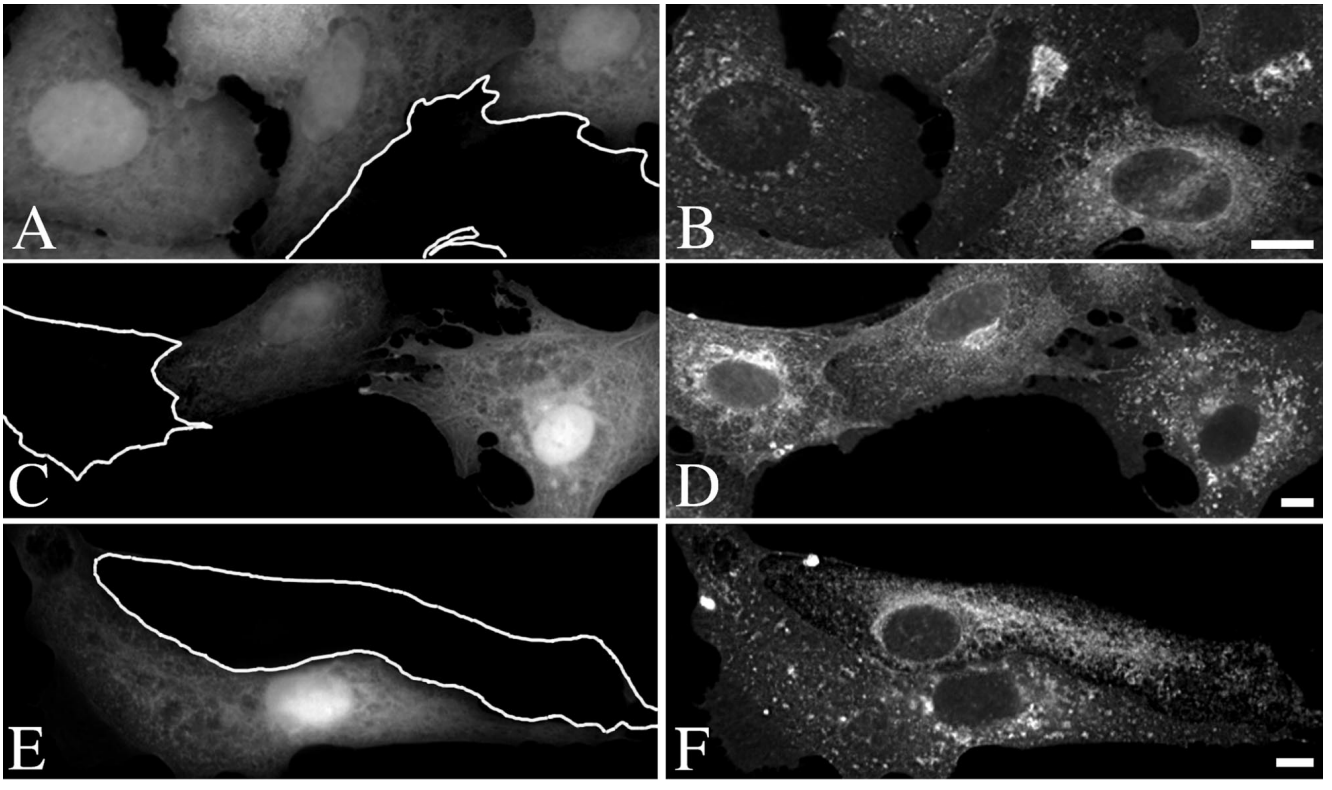

Figure 9. CT transport to the ER is inhibited by Arf1(Q71L) and Sar1(H79G). Vero cells were injected with a mixture of GFP and either Arf1(Q71L) (A and B) or Sar1(H79G) (C–F) expression plasmids and incubated in 10 μg/ml cycloheximide for 4 h. The cells were then allowed to bind and internalize CT holotoxin in the absence of cycloheximide at 20°C for 1 h and subsequently at 37°C for a further 2 h. Although the toxin (B, D, and F) clearly reached the ER in uninjected cells (outlined in A, C, and E), cells expressing the Arf1 or Sar1 mutants (identified by GFP expression shown in A, C, and E) displayed a conspicuous lack of toxin in the ER. Instead, an accumulation of the toxin in endosomes and sometimes the Golgi was observed in injected cells. Bars, 10 μm.

then association with caveolae (Anderson *et al.*, 1996; Stang *et al.*, 1997; Chen and Norkin, 1999; Norkin, 1999; Parton and Lindsay, 1999; Pelkmans *et al.*, 2001). The virus is then internalized but it is currently unknown whether the virus promotes internalization or follows the constitutive internalization of caveolae, still a contentious issue. We now show that the internalization step is blocked by BFA and by incubation at 20°C. This suggests a pathway distinct from other well-characterized internalization pathways and in particular, the constitutive entry of CT, a putative caveolar marker. Although the intracellular effects of BFA are well characterized, a role for BFA-sensitive Arf proteins in endocytic pathways at the plasma membrane has not been convincingly demonstrated. Endocytosis of CT, transferrin, and ricin have all been shown to be BFA independent (Lencer *et al.*, 1993; Nambiar *et al.*, 1993; Schonhorn and Wessling-Resnick, 1994; Uhlin-Hansen and Yanagishita, 1995). Similarly, incubation at 20°C does not inhibit CT entry and has commonly been used to accumulate ligands in early endosomes due to a block in traffic out of this compartment but not in initial internalization (Lencer *et al.*, 1992; Mallard *et al.*, 1998; Punnonen *et al.*, 1998; Ren *et al.*, 1998). Interestingly, a recent study of trafficking pathways used by various glycosyl phosphatidylinositol (GPI)-anchored proteins described a novel endocytic pathway displaying a similar sensitivity to incubation at 20°C as that of SV40 entry (Nichols *et al.*, 2001). Such a pathway was shown to convey the raft-associated proteins, GPI-anchored GFP, and an endogenous GPI-anchored protein, CD59, from the plasma membrane to a nonclassical endosomal compartment and finally to the Golgi complex (Nichols *et al.*, 2001). Another recent morphological study of the SV40 infectious pathway (Pelkmans *et al.*, 2001) demonstrated internalization of the virus to a similarly nonclassical endosomal compartment termed by the authors, the "caveosome." Common to the caveosome and the GPI-anchored protein-containing endosomal compartment is the absence of classical early endosomal markers such as EEA1 and internalized transferrin. In addition, Pelkmans *et al.* (2001) were able to demonstrate the lumenal pH of caveosomes to be neutral and also showed caveolin-1 to be a marker for this compartment. The possibility that inhibition of SV40 entry and GPI-anchored protein endocytosis at 20°C reflects an indirect effect of a block in plasma membrane delivery of key molecules trafficking through the secretory pathway rather than a direct effect on internalization still exists. Nevertheless, these pathways display key differences to known endocytic pathways and future studies will be aimed at dissecting the novel internalization mechanism.

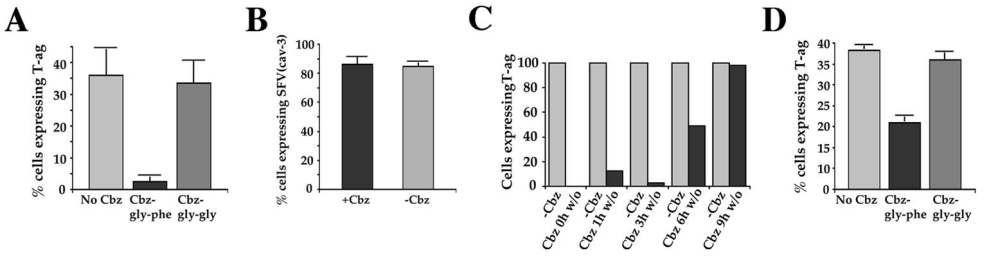

Figure 10. Cbz-gly-phe-NH2 inhibits SV40 infection but not SFV infection. (A) Vero cells were pretreated for 1 h with 2 mM Cbz-gly-phe-NH2 or its inactive analog Cbz-Gly-Gly-NH2, or were untreated. Subsequent infection with SV40 in the continued presence or absence of the dipeptides was followed by fixation and immunolabeling for T-ag. Quantitation of infection efficiency revealed a consistent inhibition of SV40 infection by the Cbz-gly-phe-NH2 but not its inactive analog. The mean and SEM of three independent experiments are shown. (B) Vero cells pretreated with 2 mM Cbz-gly-phe-NH2 for 1 h or left untreated were subjected to SFV infection in the continued presence or absence of the drug. Quantitation of infection efficiency revealed no inhibition of SFV infection in treated cells. The mean and SEM of three independent experiments are shown. (C) Vero cells were pretreated for 1 h with 2 mM Cbz-gly-phe-NH2 before a 21-h infection with SV40 in the continued presence of the drug. The cells were then washed and incubated for various periods in the absence of the drug. Although infection efficiency remained low for the first 3 h after washing out the drug, a recovery of T-ag expression began to be seen after 6 h and was complete after 9 h in the absence of the drug. Infection efficiencies are shown normalized to those of untreated controls. A representative experiment is shown. (D) Vero cells were infected with SV40 for 4 h before inactivation of surface-exposed virus by exposure to SV40 neutralizing antiserum. The cells were then incubated in medium containing 2 mM Cbz-gly-phe-NH2 or its inactive analog for a further 20 h of infection. Quantitation of T-ag expression revealed a potent inhibition of infection by the dipeptide inhibitor. The mean and SEM of three independent experiments are shown.

Involvement of Arf1, βCOP, and Sar1 in SV40 Trafficking

The most striking finding of this study is that SV40 passes from the cell surface to its site of replication via a BFA-sensitive pathway dependent on Arf1/COPI function and Sar1 function. In parallel experiments, we have shown that intracellular trafficking of cholera toxin is also sensitive to BFA, disruption of Arf1/COPI function, and disruption of Sar1 function. The block in Golgi-to-ER transport of the toxin by microinjection of anti-βCOP (EAGE) has been previously described (Majoul *et al.*, 1998). However, we herein demonstrate the inhibition of early endosome-to-Golgi transport of the toxin by BFA, βCOP antibodies, Arf1(Q71L), and Sar1(H79G). A similar inhibition of the transport of Shiga toxin (a related toxin) from early endosomes to the Golgi by BFA has been described previously (Mallard *et al.*, 1998), but the discovery of Sar1 involvement in such a pathway is unprecedented and sheds new light on the possible mechanism of inhibition. One interpretation is that Arf1 and COPI coats assembling on early endosomes mediate toxin transport to the *trans*-Golgi network (because it is well known that Arf1 mediates assembly of COP proteins on early endosomal membranes as well as Golgi membranes; Aniento *et al.*, 1996; Daro *et al.*, 1997; Gu *et al.*, 1997; Gu and Gruenberg, 2000; Jackson and Casanova, 2000). However, this does not explain Sar1(H79G)-mediated inhibition of the same step because the Sar1 GTPase is known to function only in ER-to-Golgi traffic (Aridor *et al.*, 1995). Alternatively, because Arf1/COPI function and Sar1 function are both required for anterograde transport from the ER to Golgi (Aridor *et al.*, 1995; Rowe *et al.*, 1996; Pepperkok *et al.*, 1998), it is feasible that early endosome-to-Golgi traffic is indirectly dependent on critical regulatory molecules delivered by a functional exocytic pathway. Such a dependence of endocytic pathways on a functional exocytic pathway could also explain accumulation of CT in early endosomes at 20°C, and inhibition of SV40 at the plasma membrane by BFA and at 20°C because exocytic traffic from the *trans*-Golgi network is inhibited at 20°C (Pepperkok *et al.*, 1993). Whether this reflects a need for newly synthesized caveolin-1 at the cell surface for virus internalization remains to be determined.

It is important to note that subsequent to the initial entry of the virus, an intracellular step was also found to be inhibited by BFA. The affected trafficking step in the infectious pathway still remains unresolved; electron microscopic analysis of plastic sections has proven difficult due to dramatic alteration of the morphology of intracellular compartments by the inhibitory agents used (our unpublished data). It is also possible that BFA, βCOP antibodies, Arf1(Q71L), and Sar1(H79G) are all inhibiting retrograde transport of the virus from Golgi to ER. This is however inconsistent with the findings of the Pelkmans *et al*. (2001) study, which showed an absence of colocalization of Texas Red-labeled SV40 with Golgi markers at any time during infection. Instead, live fluorescence microscopy revealed the cointernalization of the virus with GFP-tagged caveolin-1 to the caveosome compartment from where the virus was sorted away from caveolin-1 and transported along microtubule tracks to a perinuclear compartment identified as the ER by colocalization with ER markers. Our studies provide additional tools for future characterization of this as yet poorly understood infectious pathway and the molecular machinery involved.

Inhibition of SV40 Infection by Cbz-gly-phe-NH2

To further compare the properties of the SV40 and CT entry pathways, we used the dipeptide benzyloxycarbonyl Cbz-gly-phe-NH2, which has recently been demonstrated to inhibit late stages in CT toxicity (De Wolf, 2000). We now show that this drug, but not an inactive related dipeptide, is a potent and reversible inhibitor of SV40 infection. Initial characterization of the inhibition of SV40 infection showed that the drug is affecting a late stage of viral infection. Similarly, we found no apparent inhibition by the drug of early steps in uptake and delivery of CT-B-FITC to the Golgi compartment, confirming the observations of De Wolf. Infection by SFV, which enters cells via clathrin-coated pits and passes to acidic endosomal compartments before translocation to the

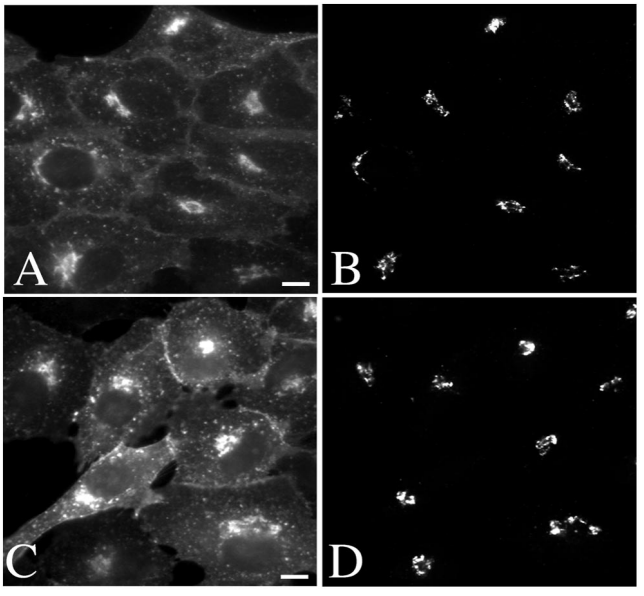

Figure 11. Post-Golgi inhibition of CT toxicity by Cbz-gly-phe-NH2. Vero cells were preincubated in 2 mM Cbz-gly-phe-NH2 (A and B) or its inactive analog (C and D) before binding and internalization of CT-B-FITC (A and C) for 40 min in the continued presence of the drugs. The cells were then fixed and immunolabeled for the Golgi matrix protein GM130 (B and D). No apparent difference in CT-B uptake to the Golgi complex was observed in inhibitor-treated cells. Bar 10 μm.

cytosol, was completely unaffected by the drug, emphasizing the specificity of the inhibition for the SV40 and CT pathways. Also, production of the membrane protein SFV-(cav-3) upon infection indicates that inhibition of protein translation was not occurring in these experiments, although such an effect of the drug has been described by others (Strous *et al.*, 1988; Brostrom *et al.*, 1991; Prostko *et al.*, 1992). Similarly, expression of a cytosolic protein, GFP, under the SV40 promoter was found to be equally competent in treated and untreated cells (our unpublished data). Thus, the inhibition of T-ag expression after SV40 infection of treated cells cannot be attributed to an inhibition of protein translation. How does this dipeptide affect SV40 infection and is it acting in a similar manner to block both CT action and SV40 infection? Cbz-gly-phe-NH2 is a metalloprotease inhibitor but the drug is known to cause depletion of intracellular stores of calcium and lowers cytosolic calcium (Brostrom *et al.*, 1991). This effect on calcium stores is thought to underlie its inhibition of membrane trafficking events between the ER and Golgi complex, and the Golgi complex and plasma membrane (Strous *et al.*, 1988; Gravotta *et al.*, 1990; Kuznetsov *et al.*, 1992; Ivessa *et al.*, 1995) and increasing extracellular levels of calcium has been found to rescue this inhibition (Kuznetsov *et al.*, 1992). However, we have found that the inhibition of SV40 infection still occurs in the presence of elevated extracellular calcium levels (our unpublished data). Identical results were obtained for the inhibition of CT toxicity by Cbz-gly-phe-NH2 (De Wolf, 2000). This is suggestive of a common mechanism of inhibition of these two processes that differs from previously described effects of the drug. It has also been suggested that Cbz-gly-phe-NH2 may affect channels involved in CT transport to the cytosol (De Wolf, 2000). This hypothesis can now be tested and may render this drug a valuable tool for dissecting the enigmatic late steps in SV40 translocation.

In summary, we have identified hitherto unexpected COP-dependent trafficking steps involved in SV40 infection. The cellular machinery and the sorting mechanisms directing SV40 along this novel route now await dissection. The tools described herein should prove powerful in further efforts to dissect, and possibly exploit, this novel viral trafficking pathway.

ACKNOWLEDGMENTS

We are indebted to Dr. Janet Butel for providing neutralizing antiserum to SV40 and to Dr. Juergen Kartenbeck for providing SV40 stocks. We are also grateful to members of the Parton laboratory for comments on the manuscript. This work was supported by a grant from the National Health and Medical Research Council of Australia (to R.G.P.) and was made possible by an equipment grant from the Wellcome Trust. A.A.R. is the holder of a University of Queensland Graduate School Research Travel Award. The Institute for Molecular Bioscience is a Special Research Center of the Australian Research Council.

REFERENCES

Anderson, H.A., Chen, Y., and Norkin, L.C. (1996). Bound simian virus 40 translocates to caveolin-enriched membrane domains, and its entry is inhibited by drugs that selectively disrupt caveolae. Mol. Biol. Cell *7*, 1825–1834.

Anderson, H.A., Chen, Y., and Norkin, L.C. (1998). MHC class I molecules are enriched in caveolae but do not enter with simian virus 40. J. Gen. Virol. *79*, 1469–1477.

Aniento, F., Gu, F., Parton, R.G., and Gruenberg, J. (1996). An endosomal beta COP is involved in the pH-dependent formation of transport vesicles destined for late endosomes. J. Cell Biol. *133*, 29–41.

Aridor, M., Bannykh, S.I., Rowe, T., and Balch, W.E. (1995). Sequential coupling between COPII and COPI vesicle coats in endoplasmic reticulum to Golgi transport. J. Cell Biol., *131*, 875–893.

Breau, W.C., Atwood, W.J., and Norkin, L.C. (1992). Class I major histocompatibility proteins are an essential component of the simian virus 40 receptor. J. Virol. *66*, 2037–2045.

Brostrom, M.A., Prostko, C.R., Gmitter-Yellen, D., Grandison, L.J., Kuznetsov, G., Wong, W.L., and Brostrom, C.O. (1991). Inhibition of translational initiation by metalloendoprotease antagonists. Evidence for involvement of sequestered Ca2+ stores. J. Biol. Chem. *266*, 7037–7043.

Butel, J.S., Wong, C., and Medina, D. (1984). Transformation of mouse mammary epithelial cells by papovavirus SV40. Exp. Mol. Pathol. *40*, 79–108.

Chen, Y., and Norkin, L.C. (1999). Extracellular simian virus 40 transmits a signal that promotes virus enclosure within caveolae. Exp. Cell Res. *246*, 83–90.

Clever, J., Yamada, M., and Kasamatsu, H. (1991). Import of simian virus 40 virions through nuclear pore complexes. Proc. Natl. Acad. Sci. USA *88*, 7333–7337.

Dangoria, N.S., Breau, W.C., Anderson, H.A., Cishek, D.M., and Norkin, L.C. (1996). Extracellular simian virus 40 induces an ERK/MAP kinase-independent signaling pathway that activates primary

response genes and promotes virus entry. J. Gen. Virol. *77*, 2173–2182.

Daro, E., Sheff, D., Gomez, M., Kreis, T., and Mellman, I. (1997). Inhibition of endosome function in CHO cells bearing a temperature-sensitive defect in the coatomer (COPI) component epsilon-COP. J. Cell Biol. *139*, 1747–1759.

Dascher, C., and Balch, W.E. (1994). Dominant inhibitory mutants of ARF1 block endoplasmic reticulum to Golgi transport and trigger disassembly of the Golgi apparatus. J. Biol. Chem. *269*, 1437–1448.

De Wolf, M.J. (2000). A dipeptide metalloendoprotease substrate completely blocks the response of cells in culture to cholera toxin. J. Biol. Chem. *275*, 30240–30247.

Girod, A., Storrie, B., Simpson, J.C., Johannes, L., Goud, B., Roberts, L.M., Lord, J.M., Nilsson, T., and Pepperkok, R. (1999). Evidence for a COP-I-independent transport route from the Golgi complex to the endoplasmic reticulum. Nat. Cell Biol. *1*, 423–430.

Gravotta, D., Adesnik, M., and Sabatini, D.D. (1990). Transport of influenza HA from the trans-Golgi network to the apical surface of MDCK cells permeabilized in their basolateral plasma membranes: energy dependence and involvement of GTP-binding proteins. J. Cell Biol. *111*, 2893–2908.

Griffiths, G., Hoflack, B., Simons, K., Mellman, I., and Kornfeld, S. (1988). The mannose 6-phosphate receptor and the biogenesis of lysosomes. Cell *52*, 329–341.

Gu, F., Aniento, F., Parton, R.G., and Gruenberg, J. (1997). Functional dissection of COP-I subunits in the biogenesis of multivesicular endosomes. J. Cell Biol. *139*, 1183–1195.

Gu, F., and Gruenberg, J. (2000). ARF1 regulates pH-dependent COP functions in the early endocytic pathway. J. Biol. Chem. *275*, 8154–8160.

Henley, J.R., Krueger, E.W., Oswald, B.J., and McNiven, M.A. (1998). Dynamin-mediated internalization of caveolae. J. Cell Biol., *141*, 85–99.

Ivessa, N.E., De Lemos-Chiarandini, C., Gravotta, D., Sabatini, D.D., and Kreibich, G. (1995). The Brefeldin A-induced retrograde transport from the Golgi apparatus to the endoplasmic reticulum depends on calcium sequestered to intracellular stores. J. Biol. Chem. *270*, 25960–25967.

Jackson, C.L., and Casanova, J.E. (2000). Turning on ARF. The Sec7 family of guanine-nucleotide-exchange factors. Trends Cell Biol. *10*, 60–67.

Kartenbeck, J., Stukenbrok, H., and Helenius, A. (1989). Endocytosis of simian virus 40 into the endoplasmic reticulum. J. Cell Biol. *109*, 2721–2729.

Kuznetsov, G., Brostrom, M.A., and Brostrom, C.O. (1992). Demonstration of a calcium requirement for secretory protein processing and export. Differential effects of calcium and dithiothreitol. J. Biol. Chem. *267*, 3932–3939.

Lanoix, J., Ouwendijk, J., Lin, C.C., Stark, A., Love, H.D., Ostermann, J., and Nilsson, T. (1999). GTP hydrolysis by arf-1 mediates sorting and concentration of Golgi resident enzymes into functional COP I vesicles. EMBO J. *18*, 4935–4948.

Lencer, W.I. (2001). Microbes, and microbial Toxins. paradigms for microbial-mucosal toxins. V. Cholera: invasion of the intestinal epithelial barrier by a stably folded protein toxin. Am. J. Physiol. Gastrointest. Liver Physiol. *280*, G781–G786.

Lencer, W.I., de Almeida, J.B., Moe, S., Stow, J.L., Ausiello, D.A., and Madara, J.L. (1993). Entry of cholera toxin into polarized human intestinal epithelial cells. Identification of an early brefeldin A sensitive event required for A1-peptide generation. J. Clin. Invest. *92*, 2941–2951.

Lencer, W.I., Delp, C., Neutra, M.R., and Madara, J.L. (1992). Mechanism of cholera toxin action on a polarized human intestinal epithelial cell line: role of vesicular traffic. J. Cell Biol. *117*, 1197–1209.

Linstedt, A.D., and Hauri, H.P. (1993). Giantin, a novel conserved Golgi membrane protein containing a cytoplasmic domain of at least 350 kDa. Mol. Biol. Cell *4*, 679–693.

Lippincott-Schwartz, J., Yuan, L.C., Bonifacino, J.S., and Klausner, R.D. (1989). Rapid redistribution of Golgi proteins into the ER in cells treated with brefeldin A: evidence for membrane cycling from Golgi to ER. Cell *56*, 801–813.

Majoul, I., Sohn, K., Wieland, F.T., Pepperkok, R., Pizza, M., Hillemann, J., and Soling, H.D. (1998). KDEL receptor (Erd2p)-mediated retrograde transport of the cholera toxin A subunit from the Golgi involves COPI, p23, and the COOH terminus of Erd2p. J. Cell Biol. *143*, 601–612.

Mallard, F., Antony, C., Tenza, D., Salamero, J., Goud, B., and Johannes, L. (1998). Direct pathway from early/recycling endosomes to the Golgi apparatus revealed through the study of shiga toxin B-fragment transport. J. Cell Biol. *143*, 973–990.

Marsh, M., Kielian, M.C., and Helenius, A. (1984). Semliki forest virus entry and the endocytic pathway. Biochem. Soc. Trans. *12*, 981–983.

Misumi, Y., Miki, K., Takatsuki, A., Tamura, G., and Ikehara, Y. (1986). Novel blockade by brefeldin A of intracellular transport of secretory proteins in cultured rat hepatocytes. J. Biol. Chem. *261*, 11398–11403.

Nakanishi, A., Clever, J., Yamada, M., Li, P.P., and Kasamatsu, H. (1996). Association with capsid proteins promotes nuclear targeting of simian virus 40 DNA. Proc. Natl. Acad. Sci. USA *93*, 96–100.

Nambiar, M.P., Oda, T., Chen, C., Kuwazuru, Y., and Wu, H.C. (1993). Involvement of the Golgi region in the intracellular trafficking of cholera toxin. J. Cell Physiol. *154*, 222–228.

Nichols, B.J., Kenworthy, A.K., Polishchuk, R.S., Lodge, R., Roberts, T.H., Hirschberg, K., Phair, R.D., and Lippincott-Schwartz, J. (2001). Rapid cycling of lipid raft markers between the cell surface, and Golgi complex. J. Cell Biol. *153*, 529–542.

Norkin, L.C. (1999). Simian virus 40 infection via MHC class I molecules and caveolae. Immunol. Rev. *168*, 13–22.

Orlandi, P.A., and Fishman, P.H. (1998). Filipin-dependent inhibition of cholera toxin: evidence for toxin internalization and activation through caveolae-like domains. J. Cell Biol. *141*, 905–915.

Parton, R.G. (1994). Ultrastructural localization of gangliosides; GM1 is concentrated in caveolae. J. Histochem. Cytochem. *42*, 155–166.

Parton, R.G., and Lindsay, M. (1999). Exploitation of major histocompatibility complex class I molecules and caveolae by simian virus 40. Immunol. Rev. *168*, 23–31.

Pelkmans, L., Kartenbeck, J., and Helenius, A. (2001). Caveolar endocytosis of simian virus 40 reveals a new two-step vesicular-transport pathway to the ER. Nat. Cell Biol. *3*, 473–483.

Pepperkok, R., Lowe, M., Burke, B., and Kreis, T.E. (1998). Three distinct steps in transport of vesicular stomatitis virus glycoprotein from the ER to the cell surface in vivo with differential sensitivities to GTP gamma S. J. Cell Sci. *111*, 1877–1888.

Pepperkok, R., Scheel, J., Horstmann, H., Hauri, H.P., Griffiths, G., and Kreis, T.E. (1993). β-COP is essential for biosynthetic membrane transport from the endoplasmic reticulum to the Golgi complex in vivo. Cell *74*, 71–82.

Pizarro-Cerda, J., Meresse, S., Parton, R.G., van der Goot, G., Sola-Landa, A., Lopez-Goni, I., Moreno, E., and Gorvel, J.P. (1998). *Brucella abortus* transits through the autophagic pathway and replicates

in the endoplasmic reticulum of nonprofessional phagocytes. Infect. Immun. *66*, 5711–5724.

Prostko, C.R., Brostrom, M.A., Malara, E.M., and Brostrom, C.O. (1992). Phosphorylation of eukaryotic initiation factor (eIF) 2 alpha and inhibition of eIF-2B in GH3 pituitary cells by perturbants of early protein processing that induce GRP78. J. Biol. Chem. *267*, 16751–16754.

Punnonen, E.L., Ryhanen, K., and Marjomaki, V.S. (1998). At reduced temperature, endocytic membrane traffic is blocked in multivesicular carrier endosomes in rat cardiac myocytes. Eur. J. Cell Biol. *75*, 344–352.

Ren, M., Xu, G., Zeng, J., De Lemos-Chiarandini, C., Adesnik, M., and Sabatini, D.D. (1998). Hydrolysis of GTP on rab11 is required for the direct delivery of transferrin from the pericentriolar recycling compartment to the cell surface but not from sorting endosomes. Proc. Natl. Acad. Sci. USA *95*, 6187–6192.

Rojo, M., Pepperkok, R., Emery, G., Kellner, R., Stang, E., Parton, R.G., and Gruenberg, J. (1997). Involvement of the transmembrane protein p23 in biosynthetic protein transport. J. Cell Biol., *139*, 1119–1135.

Rowe, T., Aridor, M., McCaffery, J.M., Plutner, H., Nuoffer, C., and Balch, W.E. (1996). COPII vesicles derived from mammalian endoplasmic reticulum microsomes recruit COPI. J. Cell Biol. *135*, 895–911.

Roy, S., Luetterforst, R., Harding, A., Apolloni, A., Etheridge, M., Stang, E., Rolls, B., Hancock, J.F., and Parton, R.G. (1999). Dominant-negative caveolin inhibits H-Ras function by disrupting cholesterol-rich plasma membrane domains. Nat. Cell Biol. *1*, 98–105.

Scales, S.J., Pepperkok, R., and Kreis, T.E. (1997). Visualization of ER-to-Golgi transport in living cells reveals a sequential mode of action for COPII and COPI. Cell *90*, 1137–1148.

Scheel, J., Pepperkok, R., Lowe, M., Griffiths, G., and Kreis, T.E. (1997). Dissociation of coatomer from membranes is required for brefeldin A-induced transfer of Golgi enzymes to the endoplasmic reticulum. J. Cell Biol. *137*, 319–333.

Schmitz, A., Herrgen, H., Winkeler, A., and Herzog, V. (2000). Cholera toxin is exported from microsomes by the Sec61p complex. J. Cell Biol. *148*, 1203–1212.

Schonhorn, J.E., and Wessling-Resnick, M. (1994). Brefeldin A down-regulates the transferrin receptor in K562 cells. Mol. Cell. Biochem. *135*, 159–169.

Smart, E.J., Ying, Y.S., Conrad, P.A., and Anderson, R.G. (1994). Caveolin moves from caveolae to the Golgi apparatus in response to cholesterol oxidation. J. Cell Biol., *127*, 1185–1197.

Stang, E., Kartenbeck, J., and Parton, R.G. (1997). Major histocompatibility complex class I molecules mediate association of SV40 with caveolae. Mol. Biol. Cell *8*, 47–57.

Strous, G.J., van Kerkhof, P., Dekker, J., and Schwartz, A.L. (1988). Metalloendoprotease inhibitors block protein synthesis, intracellular transport, and endocytosis in hepatoma cells. J. Biol. Chem. *263*, 18197–18204.

Tsai, B., Rodighiero, C., Lencer, W.I., and Rapoport, T.A. (2001). Protein disulfide isomerase acts as a redox-dependent chaperone to unfold cholera toxin. Cell *104*, 937–948.

Uhlin-Hansen, L., and Yanagishita, M. (1995). Brefeldin A inhibits the endocytosis of plasma-membrane-associated heparan sulfate proteoglycans of cultured rat ovarian granulosa cells. Biochem. J. *310*, 271–278.

Wolf, A.A., Jobling, M.G., Wimer-Mackin, S., Ferguson-Maltzman, M., Madara, J.L., Holmes, R.K., and Lencer, W.I. (1998). Ganglioside structure dictates signal transduction by cholera toxin and association with caveolae-like membrane domains in polarized epithelia. J. Cell Biol. *141*, 917–927.

Yamada, M., and Kasamatsu, H. (1993). Role of nuclear pore complex in simian virus 40 nuclear targeting. J. Virol. *67*, 119–130.